Corrections to Migdal's theorem for spectral functions: A cumulant treatment of the time-dependent Green's function

O. Gunnarsson
Max-Planck-Institut für Festkörperforschung, D-70506 Stuttgart, Germany

V. Meden and K. Schönhammer
Institut für Theoretische Physik, Universität Göttingen, D-37073 Göttingen, Germany
(Received 23 March 1994)

The electron spectral function is calculated for a model including electron-phonon coupling to Einstein phonons. The spectrum is studied as a function of the electronic bandwidth and the energy ε_k of the level from which the electron is removed. A cumulant expansion is used for the time-dependent Green's function, and the second- and fourth-order cumulants are studied. This approach is demonstrated to give accurate results for an exactly solvable two-level model with two electronic levels coupling to local phonons. For a one-band, infinite, three-dimensional model the cumulant expansion gives one satellite in the large-bandwidth limit. As the bandwidth is reduced, the spectrum calculated with the fourth-order cumulant develops multiple satellites, if ε_k is close to the Fermi energy E_F, and as the bandwidth becomes small, results similar to the two-level model are obtained. If ε_k is more than a phonon energy below E_F, the spectrum instead shows a very broad peak, due to the decay of the hole into a hole closer to E_F and a phonon. If the spin degeneracy of the electrons is taken into account, the broadening due to the decay of a hole into a hole closer to E_F and an electron-hole pair becomes important, even if ε_k is closer to E_F than the phonon energy. The validity of Migdal's theorem for A_3C_{60} (A=K,Rb) is discussed. The intersubband electron-phonon coupling is appreciable for A_3C_{60}, and it may be argued that the effective bandwidth is large. It is shown that Migdal's theorem is, nevertheless, not valid for A_3C_{60}.

I. INTRODUCTION

The treatment of the electron-phonon coupling in ordinary metals is greatly simplified for systems where Migdal's theorem[1] is valid. This theorem states that for systems where the electronic energy scale is much larger than the phonon energy scale, it is sufficient to calculate the lowest-order self-energy diagram. This diagram can furthermore be calculated using the bare electron Green's function.[1] Since the energy scale of typical metals is of the order of several eV while the phonon energies are typically only a fraction of an eV (0.01–0.1 eV), Migdal's theorem is usually assumed to be well satisfied for such systems. The electron spectral function has been extensively studied by Engelsberg and Schrieffer[2] for systems where Migdal's theorem is assumed to be valid.

For doped C_{60} compounds, A_3C_{60} (A=K,Rb), the situation is very different. The intramolecular phonons have energies extending up to about 0.2 eV, and the width of the partly occupied t_{1u} band is about 1/2 eV, according to band structure calculations.[5] It is therefore highly questionable if Migdal's theorem can be used for doped C_{60} compounds. For high-T_c compounds the applicability of Migdal's theorem has also been questioned. It is therefore desirable to include higher-order diagrams for these systems. We note, however, that it has been argued that the relevant bandwidth for A_3C_{60} is not the t_{1u} bandwidth but the width of all the π-derived bands extending over some 15 eV. It has therefore been argued that Migdal's theorem may be valid for A_3C_{60} after all. We discuss this below. Corrections to Migdal's theorem have been studied by Pietronero and Strässler in the context of the superconductivity of A_3C_{60}.[3] Corrections for two-dimensional systems have also been studied.[4]

An interesting limiting case is a system where a core level couples to bosons (phonons or plasmons). This is in some sense the opposite limit to the one above, since the dispersional width of the core level can be assumed to be zero. This limit has been extensively studied in the past.[6,7] A particular simple model is obtained if the bosons are assumed to be dispersionless (Einstein phonons). We then consider the Hamiltonian

$$H = \varepsilon_0 c^\dagger c + \omega_0 b^\dagger b + g(b^\dagger + b)(c^\dagger c - 1). \tag{1}$$

Here ε_0 is the core-level energy, ω_0 is the boson energy, and g is the electron-boson coupling. c and b are the annihilation operators for the electron and the boson, respectively. The exact spectral function ρ is a Poisson distribution of δ functions,[7]

$$\rho(\varepsilon) = e^{-(g/\omega_0)^2} \sum_{n=0}^{\infty} \frac{1}{n!} \left(\frac{g}{\omega_0}\right)^{2n} \times \delta(\varepsilon - \varepsilon_0 + n\omega_0 - g^2/\omega_0). \tag{2}$$

The spectrum has boson satellites displaced by $-\omega_0$, $-2\omega_0$, and so on towards lower energies. Calculating the self-energy to lowest order,

$$\Sigma_2(\varepsilon) = \frac{g^2}{\varepsilon - \varepsilon_0 + \omega_0 - i\eta}, \tag{3}$$

where η is an infinitesimal positive number, gives reasonable results for the main peak but it replaces all the satellites by one single satellite at some averaged energy.[6,7] If $(g/\omega_0)^2 \geq 1$, the higher satellites have an appreciable weight and the lowest-order diagram is therefore not sufficient.

It may then seem natural to calculate the self-energy to next order (fourth) in g, but this leads to problems.[8] For the model discussed above, for instance, the fourth-order self-energy has a double pole.

$$\Sigma_4(\varepsilon) = \frac{g^4}{(\varepsilon - \varepsilon_0 + \omega_0 - i\eta)^2(\varepsilon - \varepsilon_0 + 2\omega_0 - i\eta)}. \tag{4}$$

The corresponding Green's function therefore has incorrect analytical properties and the spectral function may be negative. An alternative approach is to expand the time-dependent Green's function in powers of the coupling constant,[9,8,10] and to use a cumulant expansion.[7,10] In this approach, the second-order cumulant expansion already gives the exact result for the core-level problem discussed above.[7]

To test the cumulant expansion, we first consider a two-level model, for which we can easily obtain the exact solution. Two electronic levels couple to each other via a hopping matrix element t and each level couples to a local boson with the energy ω_0 and the coupling constant g. The system has one electron. Even in the limit when t goes to zero, this problem is different from the core-level problem, in the sense that the second-order cumulant expansion does not give the exact result. This illustrates that the valence problem is more difficult than the core problem, due to the partial filling of the levels and due to the hopping of the electron between the electronic levels. By increasing t we can furthermore simulate aspects of a system with a finite bandwidth. The two-level model is therefore a nontrivial test case for the formalism. For $(g/\omega_0)^2 \leq 2$, we illustrate that the second-order cumulant expansion is rather accurate and that the fourth-order expansion gives excellent results for the two-level model.

We then apply the formalism to a continuous, three-dimensional, one-band, tight-binding model. We study the spectrum as a function of bandwidth and the momentum k or energy ε_k of the removed electron (the Fermi energy E_F is taken as zero). According to the calculations, such a system also has multiple phonon satellites for bandwidths of the order of or somewhat larger than the phonon frequency, if $-\varepsilon_k < \omega_0$ and the coupling is not too weak. As the energy of the one-particle level is lowered the spectrum broadens due to the decay of the hole into a phonon and a hole closer to the Fermi energy. As the bandwidth is increased the multiple phonon satellites disappear and only the lowest satellite remains. Introducing a spin degeneracy for the electronic levels leads to a substantial additional broadening, also for states where $-\varepsilon_k < \omega_0$. For certain sets of parameters, in particular without spin degeneracy, the approximation can give unphysical negative spectral weights for certain energies. The reasons are discussed below.

In Sec. II we present the cumulant expansion and in Sec. III some details about the calculation of the cumulants. In Sec. IV we study the two-level model and in Sec. V the continuous model. We discuss Migdal's theorem for A_3C_{60} in Sec. VI and the results are discussed in Sec. VII.

II. CUMULANT EXPANSION

We consider the time ordered Green's function

$$iG(k,t) = \langle\Phi|T[c_k(t)c_k^\dagger]|\Phi\rangle, \tag{5}$$

where c_k annihilates an electron in the state k, $c_k(t)$ is a time-dependent Heisenberg operator, $|\Phi\rangle$ is the ground state, and T is the time-ordering operator. We consider a general Hamiltonian of the type

$$H = \sum_k \varepsilon_k c_k^\dagger c_k + \sum_q \omega_q b_q^\dagger b_q + \sum_{k,q} g(q) c_{k+q}^\dagger c_k (b_{-q}^\dagger + b_q), \tag{6}$$

where b_q annihilates a boson with the energy ω_q and $g(q)$ is the electron-phonon coupling strength. We are interested in the photoemission spectrum $\rho^<(k,\varepsilon)$, which is described by $G(k,t)$ for $t \leq 0$,

$$\rho^<(k,\varepsilon) = \frac{1}{\pi}\mathrm{Im}\int_{-\infty}^{0} dt e^{i\varepsilon t + \eta t} G(k,t). \tag{7}$$

We use a cumulant expansion for the time-dependent Green's function.[11] Let us assume that the expansion of the Green's function in powers of the coupling constant g is known,

$$G(k,t) = \sum_{n=0}^{\infty} \frac{g^n}{n!} G_n(k,t). \tag{8}$$

Here

$$G_0(k,t) = \begin{cases} ie^{-i\varepsilon_k t} & \text{for } \varepsilon_k \leq E_F \\ 0 & \text{for } \varepsilon_k > E_F, \end{cases} \tag{9}$$

where $E_F = 0$ is the Fermi energy and $t \leq 0$. We therefore write the cumulant expansion as

$$G(k,t) = \begin{cases} ie^{-i\varepsilon_k t}\exp\left(\sum_{n=1}^{\infty}(g^n/n!)C_n(k,t)\right) & \text{for } \varepsilon_k \leq E_F \\ ie^{-i\varepsilon_k t}\left[\exp\left(\sum_{n=1}^{\infty}(g^n/n!)C_n(k,t)\right) - 1\right] & \text{for } \varepsilon_k > E_F. \end{cases} \tag{10}$$

For the Hamiltonian (6) the odd terms G_{2n+1} vanish. By expanding Eq. (10) and identifying terms of a given order in g one obtains

$$\frac{g^2}{2!}C_2(k,t) = \frac{g^2}{2!}\frac{G_2(t)}{ie^{-i\varepsilon_k t}} \tag{11}$$

and

$$\frac{g^4}{4!}C_4(k,t) = \frac{g^4}{4!}\frac{G_4(t)}{ie^{-i\varepsilon_k t}} - \frac{g^4}{(2!)^3}C_2^2(k,t). \tag{12}$$

For the core-level problem [Eq. (1)] we calculate the second-order diagram (1a) in Fig. 1 and, since the contribution of diagram (1b) vanishes, we obtain

$$\frac{g^2}{2!}G_2(\omega) = \left(\frac{1}{\omega-\varepsilon_0-i0}\right)^2 \frac{g^2}{\omega-\varepsilon_0+\omega_0-i0}. \tag{13}$$

Fourier transformation of $G_2(\omega)$ gives

$$\frac{g^2}{2!}G_2(t) = i(g/\omega_0)^2(e^{i\omega_0 t} - i\omega_0 t - 1)e^{-i\varepsilon_0 t}. \tag{14}$$

Dividing by $G_0(t) = i\exp(-i\varepsilon_0 t)$ yields $C_2(t)$ and the second-order cumulant expansion[7]

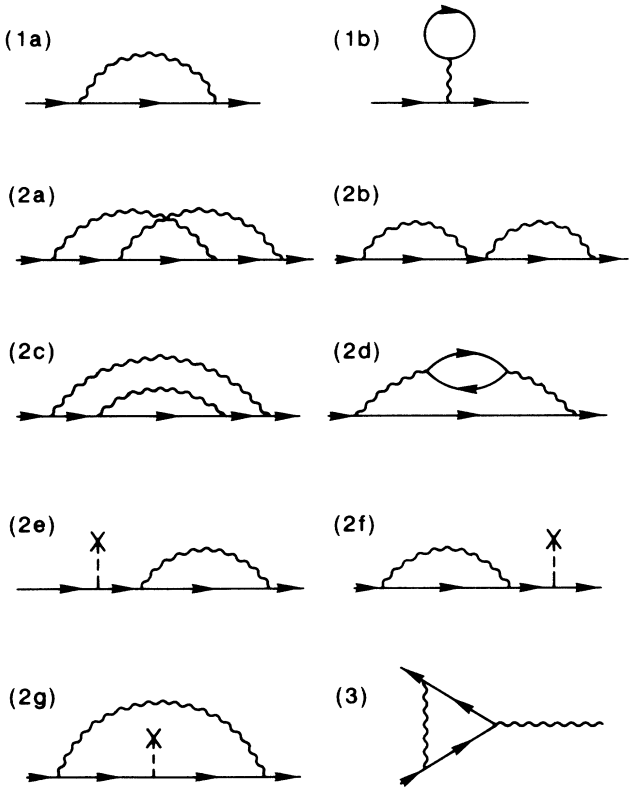

FIG. 1. Second- (1) and fourth-order (2) diagrams contributing to the cumulant expansion. The solid lines describe electrons, the wiggly lines bosons, and the dashed lines connecting to crosses describe the shift operator (40). (3) shows the lowest-order vertex correction in Eq. (45).

$$G(t) = ie^{-i\varepsilon_0 t}e^{(g/\omega_0)^2(e^{i\omega_0 t}-i\omega_0 t-1)}. \tag{15}$$

Fourier transformation of Eq. (15) leads to the exact core-level spectrum in Eq. (2). The term -1 in the parentheses in the exponent provides the prefactor $e^{-(g/\omega_0)^2}$ and the term $-i\omega_0 t$ gives the relaxation energy g^2/ω_0. Expanding $\exp[(g/\omega_0)^2 e^{i\omega_0 t}]$ gives the boson satellites. The nonzero fourth-order contribution G_4 is obtained by calculating the fourth-order diagrams (2a)–(2d) in Fig. 1, as all diagrams containing a tadpole [diagram (1b)] vanish, due to the special form of the Hamiltonian (1). When combined with $G_2(t)$ according to Eq. (14), the corresponding $C_4(t) \equiv 0$, as it should, since the second-order cumulant expansion already leads to the exact result for the core hole problem.

For the general Hamiltonian (6), the $q = 0$ coupling term gives nonvanishing tadpole contributions for finite systems. In order to avoid the corresponding abundance of diagrams, it is favorable to treat the $q = 0$ term separately. We write the Hamiltonian (6) as

$$H = H' + \omega_0 b_0^\dagger b_0 + g(0)\hat{N}(b_0^\dagger + b_0) \equiv H' + H_{q=0}, \tag{16}$$

where $\hat{N} = \sum_p c_p^\dagger c_p$ is the total number operator. Since

$$[H', H_{q=0}] = 0, \tag{17}$$

we can write the ground state for N electrons in the product form

$$|\Phi\rangle = |\Phi'\rangle|\tilde{0}\rangle, \tag{18}$$

where $|\Phi'\rangle$ is the ground-state to H' and $|\tilde{0}\rangle$ is the ground state to $H_0(N) = \omega_0 b_0^\dagger b_0 + g(0)N(b_0^\dagger + b_0)$. The ground-state energy is $E_0(N) = E_0'(N) + \tilde{E}_0(N)$. In photoemission, studied below, we use $G(k,t)$ for $t \le 0$,

$$\begin{aligned} -iG(k,t) &= \langle\Phi|c_k^\dagger e^{i[H-E_0(N)]t}c_k|\Phi\rangle \\ &= \langle\Phi'|c_k^\dagger e^{i[H'-E_0'(N)]t}c_k|\Phi'\rangle \\ &\quad\times\langle\tilde{0}|e^{i[H_0(N-1)-\tilde{E}_0(N)]t}|\tilde{0}\rangle. \end{aligned} \tag{19}$$

The first factor on the right hand side corresponds to the spectrum for the Hamiltonian H' and it is calculated using a cumulant expansion, as discussed above. The second factor can be calculated exactly[7] and we obtain

$$\begin{aligned} -iG(k,t) &= \langle\Phi'|c_k^\dagger e^{i[H'-E_0'(N)]t}c_k|\Phi'\rangle \\ &\quad\times e^{i(2N-1)\frac{g(0)^2}{\omega_0}t}e^{(\frac{g(0)}{\omega_0})^2(e^{i\omega_0 t}-1)}. \end{aligned} \tag{20}$$

For a large system, $g(0) \sim 1/\sqrt{M}$, where M is the number of sites. If $N \sim M$, only an uninteresting constant shift remains of the second factor in Eq. (20), as the size M of the system goes to infinity. For the two-level model discussed in Sec. IV this separation of the $q = 0$ term simplifies the calculations.

As a comparison, we also calculate the second-order self-energy and the corresponding Green's function and spectral function

$$\rho(k,\varepsilon) = \frac{1}{\pi}\mathrm{Im}G(k,\varepsilon) = \frac{1}{\pi}\mathrm{Im}\frac{1}{\varepsilon-\varepsilon_k-\Sigma_2(k,\varepsilon)}. \tag{21}$$

III. CALCULATION OF THE CUMULANTS

To obtain the expansion of the Green's function (8) corresponding to H', we calculate the diagrams (1a) and (2a)–(2d) in Fig. 1. We calculate the Green's functions using the Matsubara finite T formalism in the limit $T \to 0$ to obtain $G_n(k, \omega_m)$. The Green's function is then continued analytically to real frequencies, and a Fourier transformation is performed to obtain $G_n(k,t)$.

For instance, the diagram (2a) is given by

$$\frac{g^4}{4!}G_4^{(2a)}(k,\omega_m) = \frac{g^4}{\beta^2}\int\frac{d^3q}{(2\pi)^3}\int\frac{d^3q'}{(2\pi)^3}\sum_{\nu_n}\sum_{\nu_{n'}}G_0(\mathbf{k}-\mathbf{q},\omega_m-\nu_n)G_0(\mathbf{k}-\mathbf{q}-\mathbf{q}',\omega_m-\nu_n-\nu_{n'})$$
$$\times G_0(\mathbf{k}-\mathbf{q}',\omega_m-\nu_{n'})D_0(\mathbf{q},\nu_n)D_0(\mathbf{q}',\nu_{n'})G_0(\mathbf{k},\omega_m)^2, \tag{22}$$

where

$$G_0(k,\omega_m) = \frac{1}{i\omega_m - \varepsilon_k} \tag{23}$$

and

$$D_0(\mathbf{q},\nu_n) = \frac{1}{i\nu_n - \omega_0} - \frac{1}{i\nu_n + \omega_0} \tag{24}$$

are the unperturbed electron and phonon Green's functions, respectively, and $\beta = 1/T$. Since each electron Green's function provides one factor and each phonon Green's function two factors, the diagram (2a) gives four terms. In total the diagrams (2a)–(2d) give 16 terms.

We then perform the boson sums by the replacement[12]

$$\frac{1}{\beta}\sum_{\nu} \to \int_C \frac{1}{\exp(\beta z)-1}, \tag{25}$$

i.e., the frequency summation is replaced by a contour integral, where the contour C runs on both sides of the imaginary axis.[12] For the fermion sum in diagram (2d) a similar replacement is introduced. All the frequency integrals can then be performed analytically in a standard way. The number of resulting terms is, however, large, namely, 128 fourth-order terms.

We next continue the Green's function to the real axis by replacing $i\omega_m$ by the real frequency ω and perform the Fourier transform

$$G(k,t) = \int_{-\infty}^{\infty}\frac{d\omega}{2\pi}e^{-i\omega t}G(k,\omega). \tag{26}$$

Typically, $G(k,\omega)$ may have a pole of the order n at some energy ε. We are interested in photoemission and therefore in $t \le 0$. We therefore close the contour in the upper half plane. If $\varepsilon \le E_F$, where E_F is the Fermi energy, the pole corresponding to ε is located in the upper half plane and it therefore contributes to the integral. Let the behavior of $G(k,\omega)$ around $\omega = \varepsilon$ be $(\omega-\varepsilon)^{-n}f(\omega)$. Then the contribution from the pole at $\omega = \varepsilon$ is

$$i\frac{1}{(n-1)!}\frac{d^{n-1}}{(d\omega)^{n-1}}e^{-i\omega t}f(\omega)|_{\omega=\varepsilon}. \tag{27}$$

After performing these integrals, we obtain 656 terms from the diagrams (2a)–(2d).

Although these calculations are in principle straightforward, it would obviously be impractical to perform them by hand, due to the large number of terms. We have therefore written a computer program which performs these analytical integrations and generates the resulting terms, which now depend on $\varepsilon_{\mathbf{k}}$, $\varepsilon_{\mathbf{k}-\mathbf{q}}$, $\varepsilon_{\mathbf{k}-\mathbf{q}-\mathbf{q}'}$, and $\varepsilon_{\mathbf{k}-\mathbf{q}'}$. It then remains to perform the integrals over $\mathbf{q}$ and $\mathbf{q}'$. These integrals are performed using a Monte Carlo integration method.

IV. TWO-LEVEL MODEL

As a test of the formalism, we consider the two-level model

$$H = \varepsilon_0\sum_{i=1}^{2}c_i^\dagger c_i + \omega_0\sum_{i=1}^{2}b_i^\dagger b_i - t(c_1^\dagger c_2 + c_2^\dagger c_1)$$
$$+g\sum_{i=1}^{2}(b_i^\dagger + b_i)c_i^\dagger c_i. \tag{28}$$

Here $t > 0$ is the hopping between the two levels, and the separation $2t$ between the bonding and antibonding levels plays the role of the bandwidth for an infinite system. This type of model has also been studied by Ranninger and Thibblin.[13] By introducing bonding and antibonding combinations of the operators

$$c_\pm = \frac{1}{\sqrt{2}}(c_1 \pm c_2),$$
$$b_\pm = \frac{1}{\sqrt{2}}(b_1 \pm b_2) \tag{29}$$

we can transform the Hamiltonian to the standard form

$$H = \sum_{n=\pm}\varepsilon_n c_n^\dagger c_n + \omega_0\sum_{n=\pm}b_n^\dagger b_n$$
$$+\frac{g}{\sqrt{2}}[(c_+^\dagger c_+ + c_-^\dagger c_-)(b_+^\dagger + b_+)$$
$$+(c_+^\dagger c_- + c_-^\dagger c_+)(b_-^\dagger + b_-)]. \tag{30}$$

Here $\varepsilon_\pm = \varepsilon_0 \mp t$. The Hamiltonian H' without the $q = 0$ mode is given by

$$H' = \sum_{n=\pm} \varepsilon_n c_n^\dagger c_n + \omega_0 b_-^\dagger b_- + \frac{g}{\sqrt{2}}(c_+^\dagger c_- + c_-^\dagger c_+)(b_-^\dagger + b_-). \quad (31)$$

To obtain the exact spectral functions, we make the ansatz for the ground state

$$|\Phi'\rangle = \sum_{n_-=0}^{N-1} a_{n_-} c_{n_-}^\dagger |Vac\rangle |n_-\rangle, \quad (32)$$

where $|n_-\rangle$ are eigenstates of $\omega_0 b_-^\dagger b_-$ and c_{n_-} is c_+ if n_- is even and c_- otherwise. This leads to an eigenvalue problem for an $N \times N$ matrix. With increasing N this converges to the exact solution. In the final state there is no electron, and the eigenstates are of the type $|n_+\rangle|n_-\rangle|Vac\rangle$. The spectral functions $\rho_\pm(\varepsilon)$, for the bonding (+) and antibonding (−) levels, are then given by ($\beta = g^2/\omega_0^2$)

$$\rho_\pm(\varepsilon) = \sum_{n_+=0}^{\infty} \sum_{n_-=0}^{\infty} e^{-\beta} \beta^{n_+} |a_{2n_-(+1)}|^2 \times \delta\{\varepsilon + [n_+ + 2n_-(+1)]\omega_0 - E_0\}, \quad (33)$$

where (+1) applies to the antibonding (−) level and $E_0 = E_0' - g^2/\omega_0$ is the ground-state energy.

Due to the interaction with the phonons, the antibonding level is also occupied in the ground state. This level therefore contributes to the photoemission spectrum. In the $t \to 0$ limit, the sum of the spectra for the bonding and antibonding levels is identical to the spectrum for the core-level model, while the spectrum of the bonding level alone differs from the core-level spectrum.

We also calculate the second-order self-energy corresponding to the diagrams (1a) and (1b) in Fig. 1,

$$\Sigma_2(\varepsilon) = \frac{g^2}{2}\left(\frac{1}{\varepsilon + \omega_0 + t} + \frac{1}{\varepsilon - \omega_0 - t}\right) - \frac{g^2}{\omega_0}. \quad (34)$$

Inserting this result into the Green's function (21), we obtain the second-order spectral function.

In Fig. 2 we show results for the spectrum of the two-level model. We have used $\omega_0 = 0.2$ eV, which is the energy of the highest phonon in C_{60} and $g = \omega_0$, which may be a typical value for the electron-phonon coupling in C_{60}.[14] We have chosen $t = 0.05$ eV, which corresponds to a small bandwidth.

For the bonding level (lower part of figure), the second-order cumulant expansion (dashed curve) provides a rather accurate solution and the fourth-order (dotted curve) result is almost exact. Thus the agreement is within the plotting accuracy except for the two satellites below −0.5 eV. The spectrum for the antibonding level is shown in the upper part of the figure. The accuracy of this spectrum is substantially worse. The second-order result gives rather accurate weights, but the energies are less accurate than for the bonding level. The fourth-order result gives negative spectral weights, and it is in many respects worse than the second-order result.

To analyze the reason for the poor fourth-order result

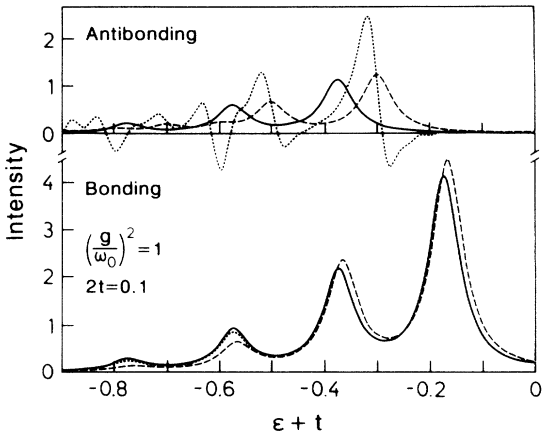

FIG. 2. The photoemission spectrum from the bonding (lower part) and antibonding (upper part) level of the two-level model. The parameters are $\omega_0 = 0.2$ eV, $(g/\omega_0)^2 = 1$, and $2t = 0.1$ eV. The energy scale has been displaced so that the peak for the bonding level would have appeared at 0 for a noninteracting system ($g = 0$). The shift operator (40) described in the text has *not* been included. The full curve shows the exact result, the dashed and dotted curves show the result of a second- and fourth-order cumulant expansion, respectively. A Lorentzian broadening with the half-width 0.035 eV has been used.

for the antibonding level, we first show the results for $C_2(t)$ and $C_4(t)$ for the bonding level. We obtain

$$\frac{g^2}{2!} G_2(+,t) = (-0.22 + 0.07it) e^{-i\varepsilon_+ t}, \quad (35)$$

which leads to

$$\frac{g^2}{2!} C_2(+,t) = -0.22 + 0.07it. \quad (36)$$

Here the term −0.22 reduces the weight of the spectrum, reflecting that in the interacting system the occupancy of the bonding level is smaller than unity. The term $0.07it$ leads to a shift of the peak, taking relaxation effects into account. The satellites in Fig. 2 are caused by the second factor in Eq. (20). The fourth-order result is

$$\frac{g^4}{4!} C_4(+,t) = -0.082 + 0.008it - 0.003(it)^2 + 0.056 e^{-i(-0.40)t}. \quad (37)$$

The first two terms slightly reduce the weights of the peaks and slightly shift them, respectively. The fourth term adds weight to the second satellite (at about −0.57 eV). For the antibonding level we obtain

$$\frac{g^2}{2!} C_2(-,t) = 0.22 e^{-i(-0.3)t}. \quad (38)$$

Expanding $\exp[C_2(-,t) - 1]$ produces the first satellite in the second-order spectrum. The energy of this satellite is not very accurate, and one may expect this to be fixed

by the fourth-order result, which is

$$\frac{g^4}{4!}C_4(-,t) = 0.015e^{-i(-0.3)t}it - 0.25e^{-i(-0.6)t}. \quad (39)$$

$C_4(-,t)$ indeed contains a term linear in it, which would have led to a shift if the factor $e^{i0.3t}$ had not been present. For the bonding level, the exponent in G multiplying the term linear in it was removed by the division by $ie^{-i\varepsilon_k t}$ in the definitions (11) and (12). For the antibonding level ε_k is above the Fermi energy, while, of course, all pieces of the spectral function contributing to photoemission are below. Thus $C_2(-,t)$ and $C_4(-,t)$ must contain exponential functions. After Fourier transformation, a function of the type $(it)e^{-i\varepsilon_a t}$ leads to a double pole at $\varepsilon = \varepsilon_a$. This results in a negative contribution to the spectral function on one side of $\varepsilon = \varepsilon_a$ and a positive contribution on the other side. This leads to a shift of a satellite located at ε_a, as desired, at least if the spectrum has some broadening. However, if the needed shift is large, and therefore the amplitude of the double pole is large, this can lead to negative pieces of the total spectral function, which is, of course, unphysical. This problem could have been avoided if we had used the prefactor $\exp(i0.3t)$ instead of $\exp(-i\varepsilon_k t)$ in the definition of the cumulant expansion [Eq. (10)] for the antibonding level. Although this approach would work for the two-level model, it would be less obvious what prefactor to use for a continuous model, which is our real interest. Thus we have not used such an approach here. The expansion could, however, be improved, even for a continuous model, by replacing ε_k by E_F in the prefactor in Eq. (10) if $\varepsilon_k > E_F$.

To avoid the problem with the double pole and to improve the second-order peak positions, we add and subtract a constant shift ε_l to the part of the Hamiltonian involving the antibonding level. Thus the level position ε_- is replaced by $\varepsilon_- - \varepsilon_l$ and we add as a perturbation the shift operator

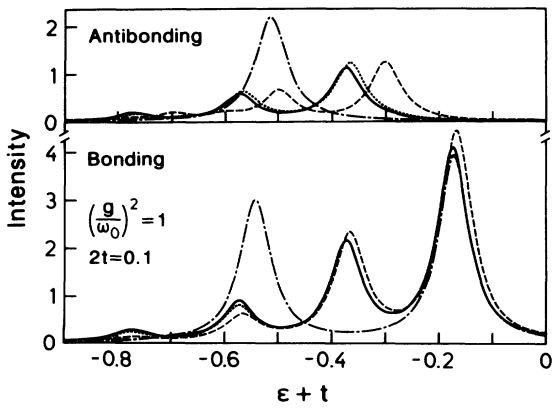

FIG. 3. Same as in Fig. 2 but with the shift operator (40) included. Also shown is the result using the second-order self-energy (dashed-dotted curve).

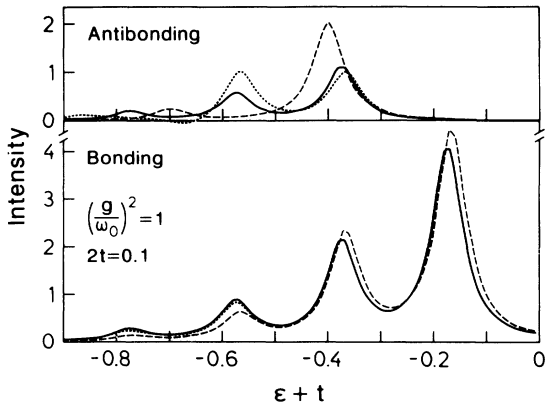

FIG. 4. Same as in Fig. 3 but treating "$\mathbf{q} = \mathbf{0}$" explicitly in the cumulant expansion.

$$\varepsilon_l c_-^\dagger c_-, \quad (40)$$

which does not change the Hamiltonian. This additional term leads to the diagrams (2e)–(2g) in Fig. 1. These diagrams also generate terms proportional to $\varepsilon_l(it)e^{-i\varepsilon_a t}$, and we can choose ε_l in such a way that terms of this type cancel. The result of such a calculation is shown in Fig. 3. For the bonding level and for the second-order calculation for the antibonding level nothing is changed, by definition. However, for the fourth-order antibonding calculation, the negative parts of the spectral function are now gone and the peak positions are greatly improved compared with the second-order calculation. The agreement with the exact solution, although not as good as for the bonding level, is quite satisfactory.

Finally, we show in Fig. 4 the result for the case when the "$\mathbf{q} = \mathbf{0}$" term is treated explicitly in the cumulant expansion and not via the last factor in Eq. (20). There is a substantial difference in the second-order cumulant result for the antibonding level between Figs. 3 and 4. In

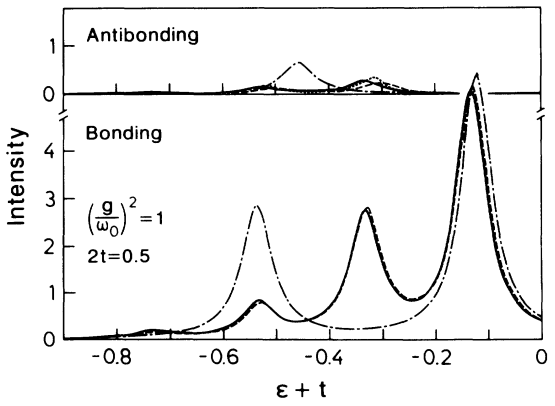

FIG. 5. Same as in Fig. 3 but with $2t = 0.5$ eV.

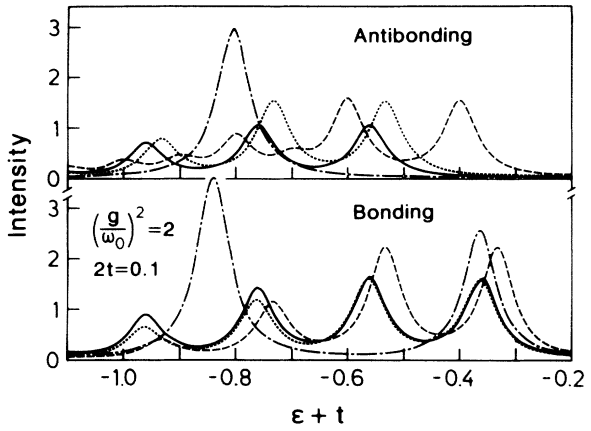

FIG. 6. Same as in Fig. 3 but with $(g/\omega_0)^2 = 2$ and $2t = 0.1$ eV.

Fig. 4 the energy of the first satellite is somewhat better but the weight is worse. For the fourth-order cumulant treatment the difference is much smaller, in particular for the first satellite. For the second satellite the result is, however, better in Fig. 3 in terms of the weight. There is a slight negative contribution to the spectral function at about -0.67 eV. This is not due to a double pole but due to a single pole with a slightly negative weight. This negative weight results from the subtraction of $(1/2)C_2^2(-,t)$ from the contribution of $G_4(-,t)$. For the bonding level there is no noticeable difference between the two treatments.

In Fig. 5 we show results for a larger splitting, $2t = 0.5$ eV, of the bonding and antibonding levels. The contribution from the antibonding level is now very small. For the bonding level the accuracy of both the second- and fourth-order cumulant expansions is excellent. The second-order self-energy gives a rather good description of the main peak for both $2t = 0.5$ (Fig. 5) and $2t = 0.1$ eV (Fig. 3), but a poor description of the satellites in both cases. For a continuous system, according to

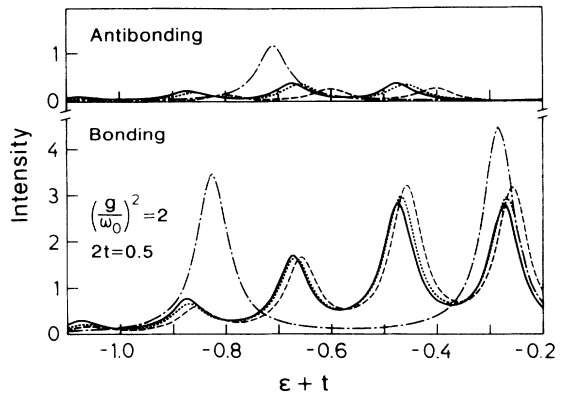

FIG. 7. Same as in Fig. 6 but with $2t = 0.5$ eV.

Migdal's theorem, the description by the second-order self-energy should improve as the bandwidth is increased, but this apparently does not happen for the discrete two-level model. Nevertheless, both the second- and fourth-order cumulant expansions become better as the "bandwidth" $2t$ is increased for the two-level model (see Figs. 3 and 5).

Figures 6 and 7 show results for a stronger coupling, $(g/\omega_0)^2 = 2$. For $2t = 0.1$ eV (Fig. 6), the second-order cumulant expansion is less accurate. The fourth-order cumulant still gives accurate results for the bonding level, while the results are less satisfactory for the antibonding level. For the larger splitting, $2t = 0.5$ eV (Fig. 7), both the second and fourth cumulant expansions are substantially improved and the fourth-order results are satisfactory for both the bonding and antibonding levels. The second-order self-energy gives a poor description of both levels for both values of t.

V. THREE-DIMENSIONAL MODEL

We have considered a Holstein model with a half-filled band, which corresponds to a Hamiltonian of the type considered in Eq. (16),

$$H = \sum_{\mathbf{k}} \varepsilon_{\mathbf{k}} c_{\mathbf{k}}^{\dagger} c_{\mathbf{k}} + \sum_{\mathbf{q}} \omega_0 b_{\mathbf{q}}^{\dagger} b_{\mathbf{q}} + \tilde{g} \sum_{\mathbf{k},\mathbf{q}} c_{\mathbf{k}+\mathbf{q}}^{\dagger} c_{\mathbf{k}} (b_{-\mathbf{q}}^{\dagger} + b_{\mathbf{q}}), \tag{41}$$

where the sums over $\mathbf{k}$ and $\mathbf{q}$ extend over the first Brillouin zone, e.g., $-\pi/a \leq k_x \leq \pi/a$. As appropriate for the intramolecular phonons of C_{60}, we have assumed that $\omega_{\mathbf{q}} \equiv \omega_0$ and $\tilde{g}(\mathbf{q}) \equiv \tilde{g}$ are independent of $\mathbf{q}$. We use a dispersion ε_k, which essentially corresponds to a nearest neighbor tight-binding model. In order to avoid a charge density instability at arbitrary weak coupling g, due to perfect nesting, we include, however, a weak next nearest neighbor hopping in the dispersion ε_k. We introduce the coupling constant

$$g^2 = \sum_{\mathbf{q}} \tilde{g}^2. \tag{42}$$

In the broad bandwidth limit, the self-energy close to the Fermi energy is proportional to g^2/B, where B is the bandwidth.[2] In this limit it is therefore sensible to keep g^2/B fixed as B is varied. In the limit of small B, on the other hand, the weights of the satellites depend on g^2, and in this limit it is more sensible to keep g^2 fixed when B is varied. Below we therefore study the spectrum as a function of B, both when g^2/B and when g^2 is kept fixed.

In Fig. 8 we show results for the spectrum as a function of the bandwidth B when g^2 is kept fixed. We have considered a one-particle level with the energy -0.05 eV relative to the Fermi energy, except for $B = 0.05$ eV, where the lowest possible level is at -0.025 eV. At the bottom of the figure, we show results for $B = 6$ eV. In this case the bandwidth is much larger than the phonon frequency $\omega_0 = 0.2$ eV. The second-order theory is very

close to the second- and fourth-order cumulants, where the latter two are identical within the plotting accuracy. For this value of B Migdal's theorem is apparently valid. As the bandwidth is reduced, the difference between the different orders increases. For $B = 1.5$ eV, a second satellite starts to form for the fourth-order cumulant and for $B = 0.6$ eV, this satellite is quite pronounced. For $B = 0.6$ eV, the result using the second-order cumulant also starts to show signs of a second satellite, which for $B = 0.05$ is very clear also for the second-order cumulant. For $B = 0.05$ there are large similarities with the results for the two-level model for a small value of t.

We observe that in Fig. 8, the spectrum becomes negative in the fourth-order cumulant solution for certain energies for $B = 0.05$ and to some extent also for $B = 0.6$ eV. This happens for somewhat similar reasons as for the antibonding level in the two-level model. Apparently the second-order cumulant places the main peak and the first satellite too close together. In the fourth-order cumulant solution, weight is subtracted to the right of an energy which roughly agrees with the satellite position and weight is added to the left. The result is a shift of the satellite towards lower energies. For $B = 0.05$ eV, so much weight is subtracted, however, that the spectrum becomes negative at some energies. The same also happens to a much smaller extent for $B = 0.6$ eV. If the one-particle level is lowered further, this effect can become quite large, and the spectrum can show large negative pieces. Although these negative pieces are clearly unphysical and signal a breakdown of the approximation, there is a clear indication in what direction the correct result is. In Fig. 8, for instance, it is clear that the satellite in the second-order cumulant result is at too high energies, and that the fourth-order cumulant tries to shift it towards lower energies.

Technically, this shows up as a contribution

$$\delta\varepsilon(-it)e^{-i(\varepsilon_k+\omega_0)t} \tag{43}$$

to the fourth-order cumulant. If the term ω_0 had not been present in the exponent, the exponent would have been divided away when calculating $C_4(t)$ according to Eq. (12). Then only a term $\delta\varepsilon(-it)$ would remain in the exponent of Eq. (10), which would result in a shift of the whole spectrum. Such a term could not cause a negative spectral weight, but it also could not change the relative separation of two peaks. Instead there are contributions of the type

$$\delta\varepsilon(-it)e^{-i\omega_0 t} \tag{44}$$

to $C_4(t)$, which, after reexpanding the exponent in Eq. (10), lead to double poles and subtraction of weight on one side of the poles and addition of weight on the other side. Such a contribution does not shift the main peak, but effectively shifts the first satellite.

In Fig. 9 we show the spectrum as a function of B,

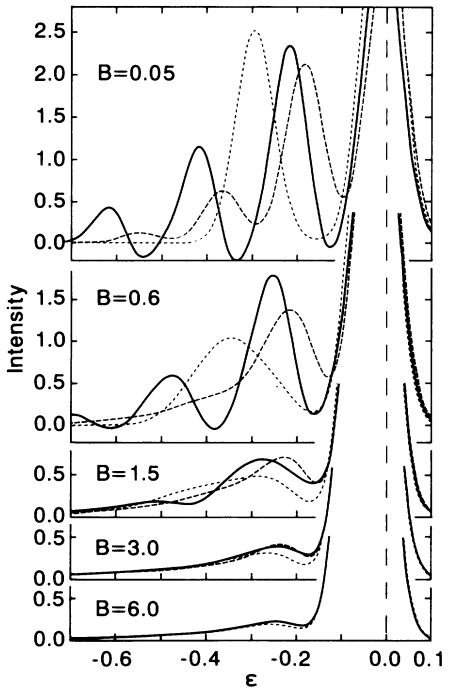

FIG. 8. Spectrum for the three-dimensional model Eq. (41), as a function of the full bandwidth B, keeping g^2 fixed. We have considered a state with the one-particle energy $\varepsilon_k = -0.05$ eV relative to the Fermi energy $E_F = 0$, except for $B = 0.05$ eV, where $\varepsilon_k = -0.025$ eV has its lowest possible value. The parameters are $\omega_0 = 0.2$ eV and $g = 0.2$ eV. We have used a Gaussian broadening with the half-width 0.05 eV. The figure shows the result using the second-order self-energy (dotted), and the second (dashed) and the fourth (full line) cumulant expansion.

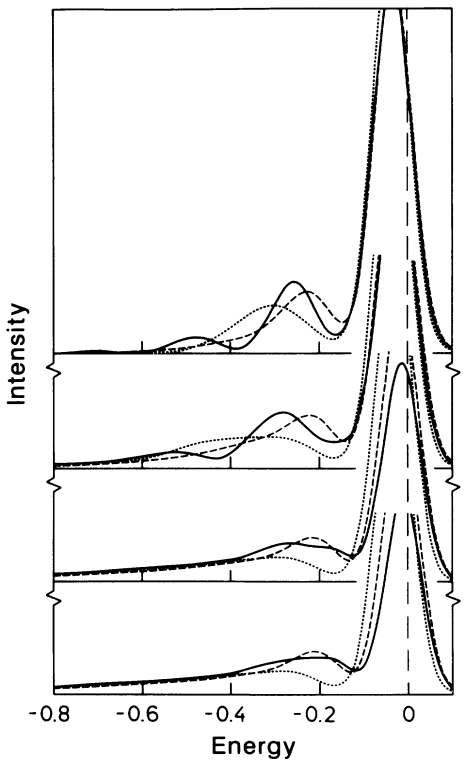

FIG. 9. Same as in Fig. 8, but keeping g^2/B fixed. We have used the value $g^2/B = 0.041$, which corresponds to $g = 0.16$ for $B = 0.6$.

when g^2/B is kept fixed. We do not show values of B smaller than 0.6 eV, since the satellites for small values of B become very small. For $B = 0.6$, the spectrum shows multiple satellites as in Fig. 8, although the satellites are weaker here. As B is increased, the multiple satellites disappear and the spectrum has only one single satellite, as in Fig. 8, although in the present case the weight of this satellite remains appreciable. The difference between the different calculations in Fig. 9 is reduced as B is increased, but the difference does not go to zero. The second- and fourth-order cumulant results are, however, rather similar. In the second- and fourth-order cumulants, the satellite has been shifted towards lower binding energies. It would be interesting to perform a self-consistent calculation of the second-order self-energy, including the dressing of the phonon Green's function, since the electron-phonon interaction should tend to reduce the energy of the pole in the phonon Green's function.

We have next considered the case when the spin degeneracy of the electrons is taken into account. This simply requires that the diagram (2d) in Fig. 1 is multiplied by a factor 2. The results are shown in Fig. 10. We have first considered a rather weak coupling $(g/\omega_0)^2 = 0.5$. We first consider $\varepsilon_k = -0.05$ eV. We can see that the main peak is substantially broader in the fourth-order cumulant expansion than in the other approximations or in the case without spin degeneracy. The reason is that the diagram (2d) allows the decay of a hole into two holes and one electron, even in the case when the hole energy is smaller than the phonon energy. This happens by exciting a virtual phonon by simultaneous scattering of the hole, followed by the decay of the phonon in an electron-hole pair. Without spin degeneracy, the broadening of the peak from diagram (2d) is to a large extent canceled by diagram (2a), but with spin degeneracy such a cancellation cannot take place due to the multiplication of diagram (2d) by a factor 2. The reason is that the broadening mechanism is not efficient if both holes have the same spin, due to exchange effects. Obviously, this broadening cannot show up in the approximation including the second-order self-energy or the second-order cumulant. As ε_k becomes more negative this broadening is increased. For $-\varepsilon_k > \omega_0$ an additional channel for broadening opens, since the hole can then decay into a phonon and a hole closer to the Fermi energy.[2] In the top part of the figure $\varepsilon_k = 0.05$ eV is above the Fermi energy, and the photoemission spectrum only shows a phonon satellite at about -0.2 eV. This spectrum has been calculated without including a linear shift of the type used for the unoccupied level in the two-level model.

In Fig. 11 we show results for a stronger coupling $(g/\omega_0)^2 = 1$. For $\varepsilon_k = -0.05$ eV, the broadening is more pronounced than in Fig. 10, due to the stronger coupling. There is still, however, a shoulder due to the first phonon satellite, which contains an appreciable weight. Already for $\varepsilon_k = -0.15$, the spectrum is so broad that no sign of a satellite can be seen, although much weight is moved towards large binding energies.

The problem of obtaining negative pieces of the spec-

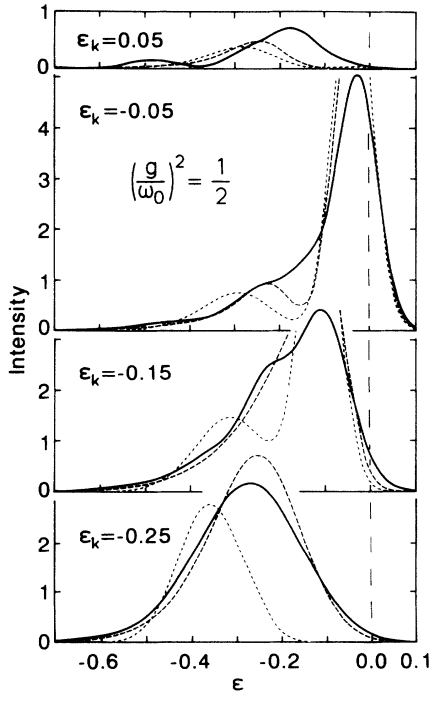

FIG. 10. Spectrum for the three-dimensional model Eq. (41), including spin, as a function of the one-particle energy ε_k. The parameters are $(g/\omega_0)^2 = 0.5$, $\omega_0 = 0.2$ eV, and $B = 0.6$ eV. The figure shows the result using the second-order self-energy (dotted), and the second (dashed) and the fourth (full line) cumulant expansion.

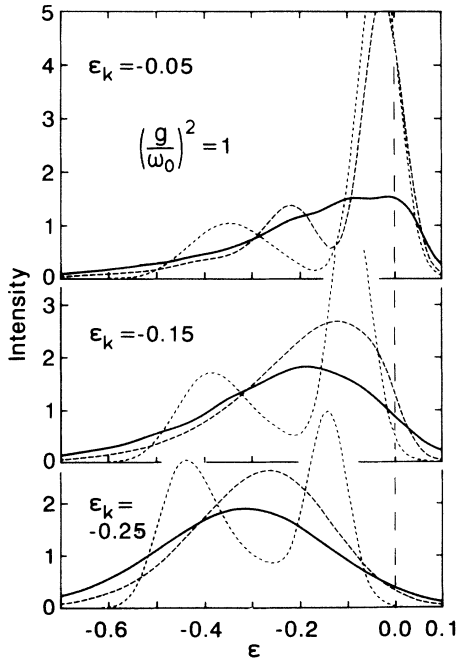

FIG. 11. Same as in Fig. 10 but with $(g/\omega_0)^2 = 1$.

tral function is greatly reduced when the spin degeneracy is introduced. This problem can, nevertheless, appear for certain parameters. For instance, for $(g/\omega_0)^2 = 1$ and ε_k close to $-\omega_0$, we have found appreciable negative contributions to the spectral function. For very small values of B we also find that the width of the spectrum is too large and the weight from the occupied part is too small.

VI. MIGDAL'S THEOREM

As mentioned in the Introduction, it has been argued that the relevant bandwidth for A_3C_{60} is not the t_{1u} bandwidth (1/2 eV), but the total width ($\sim$ 15 eV) of all the π-derived subbands, since the electron-phonon coupling connects the t_{1u} subband to all the other π-derived subbands. We have performed simple calculations of the electron-phonon coupling,[15] using an empirical model for the phonons[16] and a 60×60 tight-binding model[17] for the electronic structure. Inside the t_{1u} band the phonons of H_g symmetry give the main contribution to the electron-phonon coupling. The H_g phonons also couple the electronic state in the t_{1u} band to states in the h_u band directly below the t_{1u}. The H_g phonon, however, cannot couple the t_{1u} states to the next two bands above t_{1u} or the next two bands below the h_u band, due to symmetry reasons. There are, however, other phonons which give a coupling to these bands. We find that if all intramolecular phonons are considered, the t_{1u} band couples to all the other π-derived bands with a strength that is comparable to the coupling in the t_{1u} band itself. If we are allowed to neglect the small band gaps between the subbands, we would then arrive at the conclusion that the relevant bandwidth is large ($\sim$ 15 eV) for A_3C_{60}.

This might suggest that Migdal's theorem is actually valid for C_{60}, i.e., that the vertex corrections are small. On the other hand, it is hard to see how the vertex corrections could be large if we only consider the t_{1u} band, but would become small if we open up additional channels by considering the other subbands. Below, we show that including a few more subbands indeed makes Migdal's theorem worse, not better.

We have calculated the lowest-order vertex correction (3) in Fig. 1 using the $T = 0$ formalism. Thus we calculate the vertex function for the incoming electron energy and momentum p_0 and $\mathbf{p}$, and the incoming phonon energy and momentum q_0 and $\mathbf{q}$,

$$\Gamma_1 = i\tilde{g}^3 \int \frac{d^4k}{(2\pi)^4} \frac{1}{k_0 - \varepsilon_{\mathbf{k}} + i\eta_{\mathbf{k}}} \frac{1}{k_0 + q_0 - \varepsilon_{\mathbf{k}+\mathbf{q}} + i\eta_{\mathbf{k}+\mathbf{q}}} \times \frac{2\omega_0}{(p_0 - k_0)^2 - (\omega_0 - i\eta)^2}, \tag{45}$$

where the first two factors are electron Green's functions and the last factor is the phonon Green's function. Here η is an infinitesimal positive number and η_k is infinitesimal and positive if $\varepsilon_{\mathbf{k}}$ is above the Fermi energy and negative otherwise. Due to the very singular nature of the integrand a reliable estimate of Γ_1 and its dependence on the variables q_0, $\mathbf{q}$, and p_0 for a given value of $\mathbf{p}$ is difficult without actually performing the integral numerically. It is important to know the dependence on q_0 and $\mathbf{q}$ as one has to integrate over these variables in order to calculate the self-energy diagram (2a). In his famous attempt to obtain an order of magnitude estimate of Γ_1,[1] Migdal's main argument is that the integral over k_0 gives a large contribution if $|k_0|$ is of order ω_0 or less, and the phonon Green's function is then of order $2/\omega_0$. If we follow his arguments, we arrive at the vertex correction relative to the bare vertex ($\tilde{g}$),

$$\frac{\Gamma_1}{\tilde{g}} \sim C\frac{g^2}{B^2}, \tag{46}$$

for the model considered here, where we have assumed that the electron energies in the denominators of the two electron Green's functions typically are some fraction of the bandwidth B. The actual numerical calculations show that as a function of q_0, $\mathbf{q}$, and p_0 the vertex correction changes by an order of magnitude relative to its average value and even changes sign, where $C \sim 20$ presents an average value. We notice that Γ_1/g goes to zero as $B \to \infty$, even when g^2/B is kept constant.

These arguments illustrate how the vertex corrections become small as B increases, simply because the phonons couple to states which are increasingly far away from the Fermi energy, and therefore the energy denominators become large.

The estimates above assume that $\mathbf{q} \neq \mathbf{0}$. For $\mathbf{q} = \mathbf{0}$, the vertex function is larger,[2] and goes as g^2/B. The range of $\mathbf{q}$ where this happens is, however, not very large, at least not for large values of B. In the following we neglect the $\mathbf{q} = \mathbf{0}$ limit.

If we insert $B = 0.6$ eV and $g = 0.2$ eV, as may be reasonable for A_3C_{60}, we find that the vertex correction may be of the order 2, and that it cannot be neglected. If we now increase B, without changing the total number of states in the band, it is clear that the vertex correction rapidly becomes small, and Migdal's theorem becomes valid. This was also illustrated in Fig. 8. If, on the other hand, we increase the total bandwidth by adding extra bands, keeping the width of the t_{1u} subband fixed, we expect the vertex correction to increase.

To illustrate this, we have performed calculations for a model with three or five subbands, with the middle band half filled and the separations of the centers of the bands 1.5 eV. The results are shown in Fig. 12. The difference between the second-order self-energy calculation and the second-order cumulant expansion is unchanged as the number of bands is increased. The difference between these two calculations, on the one hand, and the fourth-order cumulant calculation, on the other hand, slightly increases with the number of bands considered, in particular, the broadening of the main peak increases somewhat with the number of bands. Thus we conclude that the validity of the assumptions behind Migdal's theorem is not improved when more subbands are taken into account.

The reason Migdal's theorem is violated in A_3C_{60} is therefore not directly related to the bandwidth, which may be argued to be large. More important is that the t_{1u} band, containing six states, has a small width (1/2

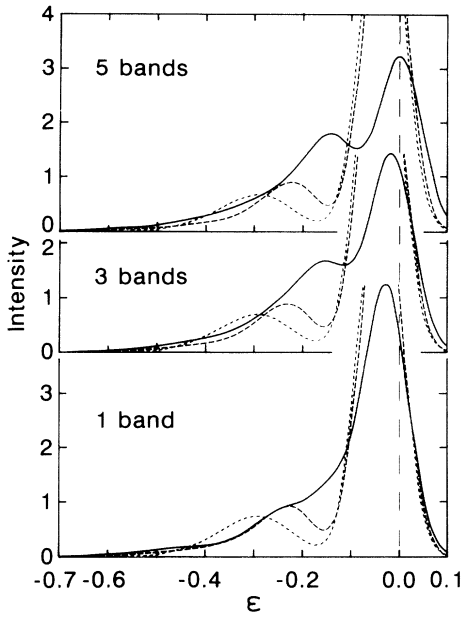

FIG. 12. Spectrum for a model with one, three, or five subbands, using the fourth- (full line) and second-order (dashed line) cumulant expansions compared with the second-order self-energy (dotted) result. The subbandwidths are 0.6 eV and the separations of their centers are 1.5 eV. The coupling is $(g/\omega_0)^2 = 0.5$ with $\omega_0 = 0.2$ eV. A Gaussian broadening with the half-width 0.05 eV has been introduced.

eV), which means that the density of states close to E_F is very large. Furthermore the coupling to t_{1u} states is relatively strong. The result is that the net coupling is so strong that vertex corrections cannot be neglected. Finally, we notice that for our one-band model, the superconductivity coupling λ is given by $\lambda = 2N(0)g^2/\omega_0$, where $N(0)$ is the density of states. Since the band takes one electron per atom in our model, we have $N(0) \sim 1/B$. Using the previous estimate Eq. (46) for the vertex correction we then find

$$\frac{\Gamma_1}{\tilde{g}} \sim 20\frac{g^2}{B^2} \sim 10\lambda\frac{\omega_0}{B}. \tag{47}$$

Thus it would be possible to have a fairly large λ but still have a small vertex correction, if $\omega_0 << B$. This is, however, not the case for A_3C_{60}.

VII. DISCUSSION

We have presented results for the photoemission spectrum for models including electron-phonon coupling. We have considered the spectra obtained from the second-order self-energy as well as from the second- and fourth-order cumulant expansions of the time-dependent Green's function. We first considered a two-level model, and showed that the fourth-order cumulant expansion gives an excellent agreement with the exact solution even for rather strong couplings $[(g/\omega_0)^2 \leq 2]$. The continuous (infinite) model is more difficult, and the accuracy of the spectra is less clear. This is, in particular, the case when the energy ε_k of the unperturbed level, from which the electron is removed, is above but close to $-\omega_0$. The second-order cumulant solution then underestimates the separation of the main peak and the first satellite. The fourth-order solution improves this separation by removing weight above the satellite and adding it below. This shifts the satellite downwards, but can lead to a negative spectral weight if the required shift is large. Nevertheless, the formalism seems to give clear indications in which direction to change the second-order cumulant solution to obtain the exact result. The problem of obtaining negative spectral weight for certain parameters is greatly reduced when the spin of the electron is taken into account.

We have first studied the spectrum as a function of the bandwidth B for the case when ε_k is close to (but below) the Fermi energy (Figs. 8 and 9). As B is increased the difference between the second-order self-energy and the fourth-order cumulant is reduced, and both spectra show only a single satellite. If, however, g^2/B is kept fixed, a finite quantitative difference remains even for very large B. As B is reduced, multiple satellites start to form in the fourth-order cumulant solution, and for small values of B, the results are qualitatively similar to those for the two-level model. It therefore seems likely that the fourth-order cumulant expansion gives a qualitatively correct picture of the dependence on B. As ε_k is moved below $-\omega_0$, the spectrum is greatly broadened (Figs. 10 and 11) due to the decay of the hole into a phonon and a hole closer to E_F. The inclusion of spin makes the decay of a hole into an electron and two holes important, even for $\varepsilon_k > -\omega_0$ (Figs. 10 and 11). This shows up as a substantial broadening even for states rather close to E_F.

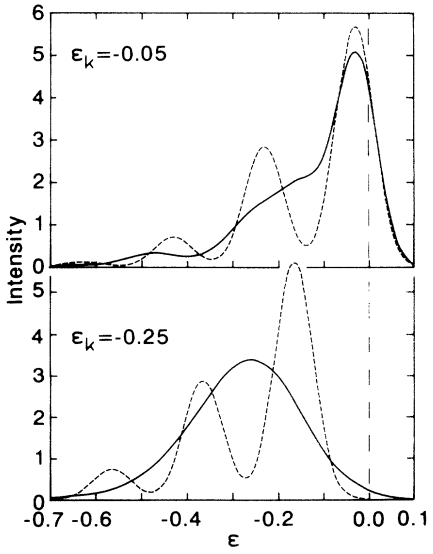

FIG. 13. Spectrum (full line) for B=0.6 eV, $(g/\omega_0)^2 = 0.5$, $\omega_0 = 0.2$ eV using the fourth-order cumulant compared with the spectrum (dashed line) from the core-level model. A Gaussian broadening with the half-width 0.05 eV was used.

Photoemission spectra from A_3C_{60} (A=K,Rb) show an unexpectedly large width for the partly occupied t_{1u} band,[18,19] which is found to be many times (approximately a factor 5) larger than what has been predicted from band structure calculations.[20] We have shown that this large width may be understood in terms of multiple phonon and plasmon satellites.[19] This was done within a model which essentially corresponds to the core-level model (1) discussed in the Introduction. This model represents an oversimplification of the real system.[19] It is therefore interesting to ask to what extent the earlier oversimplifications[19] influenced the conclusions. In particular, we have to ask how the weight at larger binding energies is influenced by the dynamics due to the band being only partly filled and having a finite width.

In Fig. 13 we show results using the fourth-order cumulant expansion for $B = 0.6$ eV and $(g/\omega_0)^2 = 0.5$ for two values of ε_k (-0.05 eV and -0.25 eV). Since there are also contributions from the levels which are unoccupied in the absence of the electron-phonon coupling, we have added the spectra for $\varepsilon_k = 0.05$ eV and $\varepsilon_k = 0.25$ eV to those for $\varepsilon_k = -0.05$ eV and $\varepsilon_k = -0.25$ eV, respectively. These spectra are compared with the results for the core-level model. As in our earlier work,[19] we have assumed that "polaronic effects" shift the main peak towards the Fermi energy, and considered energies of the order $\varepsilon_k/[1 + (g/\omega_0)^2]$. Thus we have placed the main peak at -0.03 eV and -0.17 eV, respectively, in the two "core-level" spectra. As expected, for the band model the spectra are broadened, in particular for $\varepsilon_k = -0.25$ eV, where the hole can decay in a phonon and a hole closer to the Fermi energy. It therefore seems unlikely that the individual phonon satellites can be resolved experimentally. The shift of weight towards higher binding energies due to satellites is, however, similar in the two spectra. Thus the centers of gravity are at -0.12 eV (band case) and -0.13 eV (core case) in the upper part of the figure and -0.28 eV (band case) -0.26 eV (core case) in the lower part. These results are therefore consistent with our earlier interpretation that phonon and plasmon satellites cause the large width of the photoemission spectrum in A_3C_{60}.[19]

[1] A.B. Migdal, Zh. Eksp. Teor. Fiz. **34**, 1438 (1958) [Sov. Phys. JETP **7**, 996 (1958)].

[2] S. Engelsberg and J.R. Schrieffer, Phys. Rev. **131**, 993 (1963).

[3] L. Pietronero and S. Strässler, Europhys. Lett. **18**, 627 (1992).

[4] V.N. Kostur and B. Mitrovic, Phys. Rev. B **48**, 16 388 (1993).

[5] For a review of C_{60}, see, e.g., W.E. Pickett, in *Solid State Physics: Advances in Research and Applications*, edited by H. Ehrenreich and F. Saepen (Academic, New York, 1994), Vol. 48, p. 226.

[6] B.I. Lundqvist, Phys. Kondens. Mater. **9**, 236 (1969).

[7] D. Langreth, Phys. Rev. B **1**, 471 (1970).

[8] P. Minnhagen, J. Phys. C **7**, 3013 (1974); **8**, 1535 (1975).

[9] B. Bergersen, Can. J. Phys. **51**, 102 (1973).

[10] L. Hedin, Phys. Scr. **21**, 477 (1980).

[11] R. Kubo, J. Phys. Soc. Jpn. **17**, 1100 (1962).

[12] A.L. Fetter and J.D. Walecka, *Quantum Theory of Many-Particle Systems* (McGraw Hill, New York, 1971).

[13] J. Ranninger and U. Thibblin, Phys. Rev. B **45**, 7730 (1992).

[14] V.P. Antropov, O. Gunnarsson, and A.I. Liechtenstein, Phys. Rev. B **48**, 7651 (1993).

[15] O. Gunnarsson, K. Schönhammer, and V. Meden, *Proceedings of the International Winterschool on Electronic Properties of Novel Materials, Kirchberg, 1994*, edited by H. Kuzmany, J. Fink, H. Mehring, and S. Roth (Springer, Heidelberg, in press).

[16] Z.C. Wu, D.A. Jelski, and T.F. George, Chem. Phys. Lett. **137**, 291 (1987); D.E. Weeks and W.G. Harter, *ibid.* **144**, 366 (1988).

[17] O. Gunnarsson, S. Satpathy, O. Jepsen, and O.K. Andersen, Phys. Rev. Lett. **67**, 3002 (1991).

[18] C.T. Chen, T.J. Tjeng, P. Rudolf, G. Meigs, J.E. Rowe, J. Chen, J.P. McCauley, Jr., A.B. Smith III, A.R. McGhie, W.J. Romanow, and E.W. Plummer, Nature (London) **352**, 603 (1991); P.J. Benning, F. Stepniak, D.M. Poirier, J.L. Martins, J.H. Weaver, L.P.F. Chibante, and R.E. Smalley, Phys. Rev. B **47**, 13 843 (1993).

[19] M. Knupfer, M. Merkel, M.S. Golden, J. Fink, O. Gunnarsson, and V.P. Antropov, Phys. Rev. B **47**, 13 944 (1993).

[20] S. Satpathy, V.P. Antropov, O.K. Andersen, O. Jepsen, O. Gunnarsson, and A.I. Liechtenstein, Phys. Rev. B **46**, 1773 (1992).